

**THE IMPACT OF CeO₂ ENGINEERED NANOMATERIALS ON THE
SOIL-WATER HOLDING PROPERTIES: A PEDOSTRUCTURE
CHARACTERIZATION APPROACH**

An Undergraduate Research Scholars Thesis

by

VICTORIA ELIZABETH CHAVEZ

Submitted to the Undergraduate Research Scholars program at
Texas A&M University
in partial fulfillment of the requirements for the designation as an

UNDERGRADUATE RESEARCH SCHOLAR

Approved by Research Advisor:

Dr. Amjad Assi

May 2018

Major: Civil Engineering

TABLE OF CONTENTS

	Page
ABSTRACT.....	1
DEDICATION.....	2
ACKNOWLEDGMENTS	3
NOMENCLATURE	4
CHAPTER	
I. INTRODUCTION	5
Global Perspective	5
Soil Aggregates.....	5
Soil Water Relationship	6
Nanomaterials	8
Water Reuse.....	9
Nanoparticles and Health.....	10
Objectives	11
II. METHODS	13
Pre-Laboratory Work.....	13
Laboratory Work.....	14
Calculations.....	19
III. RESULTS	21
Control	21
Three Cycles	23
Six Cycles	26
Twelve Cycles	28
IV. CONCLUSION.....	32
REFERENCES	34

ABSTRACT

The Impact of CeO₂ Engineered Nanomaterials on the Soil-water Holding Properties: A Pedostructure Characterization Approach

Victoria Elizabeth Chavez
Department of Civil Engineering
Texas A&M University

Research Advisor: Dr. Amjad Assi
Department of Biological and Agricultural Engineering
Texas A&M University

With the increase in the demand for food and clean water, non-conventional water reuse has taken a lot of attention recently. However, the impact of the reused water is still being researched. A widely used variety of engineered nanomaterials (ENMs) have been used in industry and end up in our wastewater treatment systems and therefore the environment. Studies previously conducted focused only on the implication of the nanoparticles on the plant rather than the soil. Understanding how the ENMs affect the soil aggregates will help better evaluate the soil-water holding properties, the soil health, and the soil functionality. In my research, the soil-water holding properties will be identified based on the soil aggregates structure (pedostructure approach) rather than soil texture. This research studies how a specific negatively charged engineered nanoparticle: CeO₂-NPs⁻, can alter the hydro-structural properties of a sandy soil. The results show that CeO₂-NPs⁻ have improved the soil-water retention of the studied sandy soil and increased its available water from 0.033 (kg_{water}/kg_{soil}) to 0.100 (kg_{water}/kg_{soil}). The research outcomes will contribute to better irrigation management practices as well as soil and water conservation practices.

DEDICATION

I dedicate this undergraduate research thesis to my best friends Angela, Shalie, and Caity, as well as my roommate Helen. Without their constant words of encouragement and their expectation for me to do my best and work hard at everything I do, my work would have never been possible.

ACKNOWLEDGEMENTS

I would like to thank my assisting professor, Dr. Assi, for his guidance, support, and patience with me throughout the course of this research. I would also like to thank Sonja Loy for taking me under her wing and teaching me all about the lab and about transitioning from a regular undergrad into a researcher prepared for life after college. In addition, special thanks to Mary Schweitzer who saw potential in me from the beginning and guided me through the process when I was unsure of myself.

Thanks also go to my colleagues and the Civil and Biological and Agricultural Engineering department faculties and staffs for continuing to make my undergraduate education at Texas A&M University a knowledgeable experience. I also want to thank the Milican Reserve owners whose land I extracted the undisturbed soil samples from. Without their approval and generosity, none of the following research would be possible.

Finally, thanks to my father, mother, and siblings for their encouragement to always do my best and strive for success.

NOMENCLATURE

WRC	Water Retention Curve
ShC	Soil Shrinkage Curve
NPs	Nanoparticles
NPs ⁻	Negatively charged Nanoparticles
ENPs	Engineered Nanoparticles
ENMs	Engineered Nanomaterials
BAEN	Biological and Agricultural Engineering
CVEN	Civil Engineering
TAMU	Texas A&M University
CeO ₂	Cerium Oxide
FC	Field Capacity
PWP	Permanent Wilting Point

CHAPTER I

INTRODUCTION

Global Perspective

Water and food security are among the top challenging issues in the globe today. The Agricultural sector itself consumes more than 70% of the global freshwater to feed more than 7 billion inhabitants and the number continues to increase. With the increasing demand on water and food, many challenges are imposed in managing agricultural production such as the amount of freshwater that needs to be allocated for domestic uses which in turn, reduces the available water for agricultural production. Soil plays a pivotal role in water and food security. Soil health and productivity need to be considered in managing any agro-environmental practices in agricultural production systems. Therefore, the scientific community needs to: (1) identify sustainable (re)use of new sources of water and non-conventional water such as wastewater and greywater, to bridge the water demand gap; (2) improve the water-use efficiency in agricultural production, and most importantly; and (3) reduce the impact of these human and agro-environmental interventions on soil health and productivity.

Soil Aggregates

Soil is a main component in any agricultural system. It consists of solid particles of different sizes (sand, silt and clay), which when combined together under certain conditions form soil aggregates. Soil aggregates are a key indicator for soil health, and hence, need to be considered in identifying the soil-water holding properties (Braudeau, Sene, Mohtar, et al., 2005). Currently, most of the methods used in calculating the soil-water holding properties are based on the soil texture rather than the soil aggregates structure. Actually, the agro-

environmental interventions will not change the soil texture but rather change the soil aggregates structure. Thus, it is imperative to understand how these interventions alter the soil aggregates structure and hence the soil-water holding properties for better agriculture water management.

Soil aggregates will have different characteristics based on what kind of soil they are and how the soil particles of this soil (sand, silt and clay) aggregate together. For instance, if it is a clayey soil with high organic matter, the aggregates will have a higher water retention because the clay surface particles have a negative charge that the hydrogen atoms from the water molecules wants to hold on to. A sandy soil, however, does not have as strong a surface charge and does not form a good aggregate, so there is more space between the aggregates for water to drain through. “Persistence, sorption and uptake behavior... [varies] across soil types,” (Anuar and Firdaus, 2016).

Soil-Water Relationship

Soil-water relationships are usually characterized through two characteristic curves: the soil water retention curve (WRC) and the soil shrinkage curve (ShC). WRC is the relationship between the soil water content and soil suction, hence this curve provides information about the ability of soil to hold water and how tightly the soil can hold water. ShC is the relationship between the soil water content and the soil volume, and hence describes the aggregates structure of the soil medium. Among the soil-water holding properties are the Field Capacity (FC), the Permanent Wilting Point (PWP), and the Available Water Capacity (AW). The Field Capacity is “the amount of water held in the soil after excess water has drained away and the rate of downward movement has materially decreased,” (Veihmeyer & Hendrickson, 1931) and the Permanent Wilting Point is the point at which water can no longer be reached by plant roots. Available Water Capacity is the amount of water in the soil that the plant is able to use and is,

therefore, the difference between the Field Capacity and the Permanent Wilting Point. These properties can be identified from the two characteristic curves, and they are important properties for irrigation management (Zacharias and Bohne, 2008). Therefore, better quantification of the soil-water holding properties is imperative for better use of water resources: when, how much and how often to irrigate.

As mentioned earlier, the soil-water holding properties are currently identified based on the soil texture (percent of sand, silt and clay in a soil medium) (Allen et al., 1998). However, according to Mohtar et al. (2015), soil aggregate structures should be considered in identifying the soil-holding properties for two reasons: (1) soil aggregates are a functional identity for soil mediums and tell a lot about soil health, and (2) tracking the changes in soil health due to the agro-environmental practices cannot be done through the soil-texture, but through the changes in the soil aggregates structure.

Braudeau et al. (2014, 2016) introduced the pedostructure approach to characterize the soil aggregates structure through a set of hydro-structural properties that can be identified from the measured soil-water characteristic curves: water retention curve (WRC) and soil shrinkage curve (ShC). Assi et al. (2014) provided a methodology for extracting the hydro-structural properties from the measured WRC and ShC by a state-of-art apparatus (TypoSoil™). These hydro-structural properties can be used to: (1) identify the soil-water holding properties (Assi et al., 2018, submitted); and (2) track the changes in the soil aggregates structure and hence the changes in soil-water holding properties. This research will use the pedostructure approach to track the changes in the soil-water holding properties (FC, PWP, and AW) due to the exposure to CeO₂-NPs.

Nanomaterials

Nanomaterials and nanoparticles are normally less than 100 nanometers in size. Engineered nanoparticles have recently been used in many applications including paint coatings, sunscreen, cosmetics, microelectronics, catalysts, and fuel additives (Ma et al., 2015). They also play a part in the manufacturing and packaging of many foods such as powdered sugar, coconut, and yogurt (all of which from Titanium Dioxide nanoparticles). Engineered Nanoparticles are usually coated with materials that can have positive or negative charges and can thus alter the water retention in the soil medium hence affecting the soil-water holding properties.

Nanomaterials and Civil Engineering

Nanomaterials are very helpful with modifying materials to improve their "...wettability, viscosity, seep efficiency and surface attraction forces," (Zheng, 2016). This is specifically helpful with Geotechnical Engineering and Civil Engineering when dealing with materials that need certain specifications. In addition, "Building materials can be one of the main beneficiaries of [nanomaterial] researches, with applications that will improve the characteristics of concrete, steel, glass," (Olar, 2017). Olar goes on to express that "improving the materials resistances and the increasing of their durability..." will help to reduce environmental pollution through the reduction of carbon emission for the buildings.

In construction, the "addition of nanoscale materials into cement could improve its performance. Use of nano-SiO₂ could significantly increase the compressive for concrete, containing large volume fly ash...and improve pore size distribution by filling the pores," (Padmanabhan, 2014). Plus, because they are nano-scaled, they do not add much weight to the structure. The additions of specific nanoparticles can even increase compressive and flexural strength or fix cracks in some structures. Applications of nanoparticles in civil engineering allow

materials to increase strength and boundary properties. Nanoparticles have allowed civil engineers to create high-performance steels and Titanium Oxide (TiO₂) hydrophilic coats that allow water to spread evenly over the surface of the material and wash away excess dirt, as well as sensors that help monitor the condition and performance of many construction devices.

Nanomaterials and Environmental Engineering

Environmental nanotechnology is used for the study of potential environmental, health, and safety risks. “Nanomaterials and nanoparticles pose as a threat as potential environmental pollutants due to their continual release,” (Feriancikova, 2014) usually through water because they can potentially stay in the water even with many filtering processes due to their size. However, nanomaterials also “have the potential for their application in environmental remediation, water purification and products recycling and recovery” (Oyanedel, 2016) because of their chemical and physical properties.

Charge qualities of the nanoparticles may also help humans because when combined with a substance with an opposite charge, the nanoparticles may act as a strengthening tool or glue to aid with liquid retention or flow. This specific application may allow engineers to create better retention ponds in areas with soil that would normally take more synthetic materials to have the same effect as a soil with a better ability to hold water such as a clayey soil would.

Water Reuse

Non-conventional water reuse, such as wastewater and greywater, can bridge the gap in fresh water supply. However, non-conventional water can also have a negative impact on soil health and productivity (Belhaj et al., 2016). In this research, the focus will be on one component in wastewater that is expected to gain more attention due to the increase in usage and the

associated potential, impact on soil, plants, and consequently human health. This component is the engineered nanoparticles.

Nanoparticles and Health

With the recent wide spread use of nanoparticles, the question of how they affect our health has not yet been answered. Researchers on “Nanofood” have been addressing the concern of the nanoparticles accumulating in tissues and organs inside the consumer who eats the food with nanoparticle treatment due to the size of the particles inserted in the foods.

In 2014, Cyren M. Rico did a study on the effects of cerium oxide nanoparticles in cereals and found that the nanoparticle impacted the growth and productivity of the specific cereals chosen. Part of Rico’s conclusion stated: “The NP can enhance Ce accumulation in grains and possibly compromise their nutritional value,” but there was no definite answer of what the cerium oxide nanoparticle-affected cereal would have on human or animal health.

When looking at effects of nanoparticles on human health, there are few models that help put the data in perspective. One of which is a physiologically based pharmacokinetic (PBPK) model, which “successfully predicts the dynamics of...nanoparticles between and within organs. According to the model, phagocytizing cells (PCs) quickly capture nanoparticles until saturation and constitute a major reservoir for nanoparticles,” (Li, 2015). Li uses the PBPK model in order to predict the effect of cerium oxide nanoparticles in human organs (via rats). Later Li acknowledges, “PCs in the pulmonary region are accountable for most of the nanoparticles not eliminated by feces.” Therefore, it is important that any and all engineered nanoparticles used should be known to pose potential harm if anyway ingested. This does not mean that all nanoparticles will have a negative effect, but we should always be careful because the risk exists.

Many scholars understand that there has been an increased use of *nanoengineered* materials in consumer products and this "...will result in the release of nanomaterials into natural and environmental compartments (water, air, soil)," (Craver, 2016). Oyanedel-Craver's material even exposes that some nanoparticles can have negative effects on fish, bacteria, and human cell cultures. Nanoparticles and nanomaterials may positively or negatively impact everything around us, and much research has explored the effects on plants, but little has been researched on the effect on soil which in turn affects the water circulation, flow and most importantly the agriculture water management.

Objectives

My research studies the changes in soil-water holding properties through characterization of the soil hydro-structural properties of a sandy soil by comparing a controlled sandy soil with no addition of cerium oxide nanoparticles ($\text{CeO}_2 \text{ NPs}^-$) with sandy soil samples with different amounts of two concentrations of negatively charged $\text{CeO}_2 \text{ NPs}^-$. My process tracks the changes in the soil-water holding properties, which are due to the nanoparticles (cerium oxide nanoparticles ($\text{CeO}_2 \text{ NPs}^-$) in wastewater, for example.

The overall objective is to better understand the role of soil texture and aggregates structure in identifying the soil-water holding properties and soil-water conservation practices. Specifically, this study will evaluate the effect of negatively charged cerium oxide nanoparticles ($\text{CeO}_2 \text{ NPs}^-$) on the soil hydro-structural properties and soil-water holding properties of a sandy soil.

Since my soil samples type is sandy and I am adding negatively charged nanoparticles, I expect the soil's hydrostructural properties to behave like that of a clay soil, i.e. increase the soil-water retention.

Finally, it is worth mentioning that this research is a continuation of an ongoing research initiative in the water-food-energy nexus research group and was originally pursued by a now-PhD candidate, Britany Hallmak, so my part of my method and the numbers for things like the concentrations of CeO₂ NPs- were chosen in order to eventually compare my data of sandy soil with her data of clayey soil.

CHAPTER II

METHODS

In this chapter, I will go through the processes in which I conducted my research including the experiment setup, soil extraction, the use of the Civil Engineering Laboratory, the use of the Biological and Agricultural (BAEN) Engineering Pedostructure Characterization Lab, and the steps taken to receive results.

Pre-Laboratory Work

Setup

To begin, I determined how many samples of soil and how much CeO_2 NP⁻ solution to prepare. Since my work is a continuation of Britany Hallmak's, my experiment used a similar saturation cycle system to increase the concentration of CeO_2 NP⁻ in the soil samples by adding cerium oxide nanoparticle solution multiple times until reaching the required concentrations. Specifically, nanoparticle concentrations of 0 mg/L (the control), 500 mg/L, and 2000 mg/L were used. Each of the concentrations besides the control has three soil samples exposed to three cycles, three samples exposed to six cycles, and three samples exposed to twelve cycles where one cycle is the addition of 50mL CeO_2 . For example, after three cycles of the 500 mg/L concentration there are 150 mL of CeO_2 . After three cycles of the 2000 mg/L concentration there are 6000 mg/L and 150 mL of CeO_2 . By this information and Table 1, I concluded that I needed at least eighteen soil cores, 5L of the 500mg/L solution, and 5L of the 2000 mg/L solution in order to conduct my experiment.

Table 1. Concentration of CeO₂ NP⁻ Solution and the Number of Cycles for Each Sample

	0 mg/L	500 mg/L	2000 mg/L
3 cycles	■ ■ ■	■ ■ ■	■ ■ ■
6 cycles		■ ■ ■	■ ■ ■
9 cycles		■ ■ ■	■ ■ ■

Note: ■ represents an individual soil sample. The soil samples for the same concentration are added onto and not replaced.

Soil Collection

The BAEN Pedostructure Characterization Laboratory is a busy place, so I waited my turn to gather enough empty soil cores to conduct my fieldwork during the fall semester. Finally, on December 7th, 2017 a graduate student, Sonja Loy, and I headed out to Milican Reserves, College Station, TX 77845 with enough empty cores to retrieve my soil samples. At noon we extracted the soil samples from a field plot (Latitude 30.4942, Longitude -96.2417), from the Ap Horizon of Chazos loamy fine sand soil. We were in the “Garden” of Milican Reserve collecting fine sand soil samples (texture: 4% clay, 13% silt, and 83% sand).

Laboratory Work

Civil Engineering

Dr. Samuel Ma and Xiaoxuan Wang of the CVEN department (TAMU) assisted me in preparing the cerium oxide solutions, which would be added to the soil samples and dried in the BAEN Pedostructure Characterization Laboratory. To do this, we put on gloves and retrieved a 500 mL graduated cylinder and two storage containers (for the 500 mg/L and the 2000 mg/L), each holding approximately 0.9 L. In each storage bottle I poured 900mL of water and added the

cerium oxide¹ to the appropriate bottles: 7.45 mL CeO₂ to the “2000 mg/L” bottle and 1.90 mL CeO₂ to the “500mg/L” bottle. Then, Dr. Ma instructed me to stir the CeO₂ solutions in the bottle before applying to the soil samples in order to evenly distribute the CeO₂ in the water to obtain the best and most consistent results.

Biological and Agricultural Engineering (Pedostructure Characterization Laboratory)

After making the cerium oxide solutions, they were carried to the Pedostructure Characterization Laboratory at BAEN. At the lab, the experimental setup was ready as shown in Figure 1. The figure represents the layout of the back two tables, on which are the majority of tools I used. Spot E of Figure 1 is a case of the soil cores numbers 65-72. These cores are the control samples. Spot D is a box with the two bottles: “500 mg/L” and “2000 mg/L” CeO₂ solution. Locations C and F are the soil cores prepped with duct tape (for a barrier to keep the CeO₂ NP⁻ solution from leaking), sitting on filter paper and raised on mesh file folder holders in order to naturally dry the cores. The soil cores at C are numbered 49-56 and are for the “500 mg/L” runs and the cores at F are numbered 57-64 for the “2000 mg/L” experiment. On the left side of the table sits the oven (A) and the 8 sand saturation stations (B).

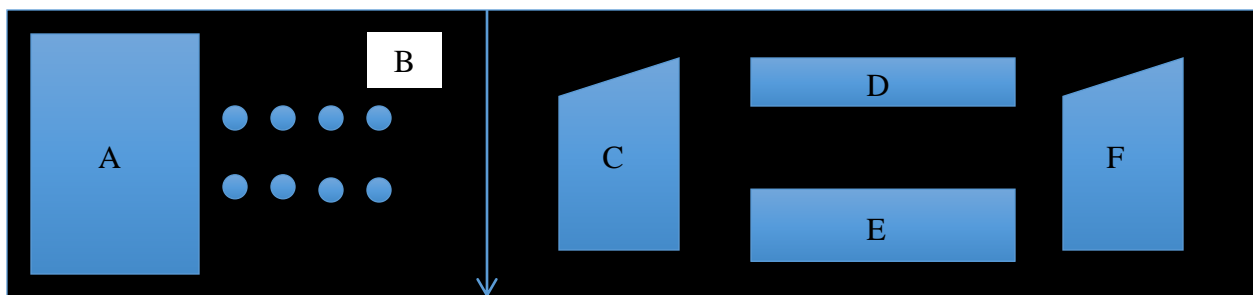


Figure 1: Layout of Tables in BAEN Pedostructure Characterization Laboratory.

¹ Cerium Oxide Nanopowder Water Dispersion (CeO₂, 20wt%, 30-50nm)

Within the Pedostructure Characterization Laboratory in the BAEN department is a unique machine known as the TypoSoil™ (Figure 2b). This machine analyzes soil cores using special sensor and tensiometer technology. As a one-of-a-kind machine in the USA, the TypoSoil™ measures simultaneously and continuously the three state variables of a soil-water medium: water content, soil suction, and soil volume for 8 soil samples at a time.

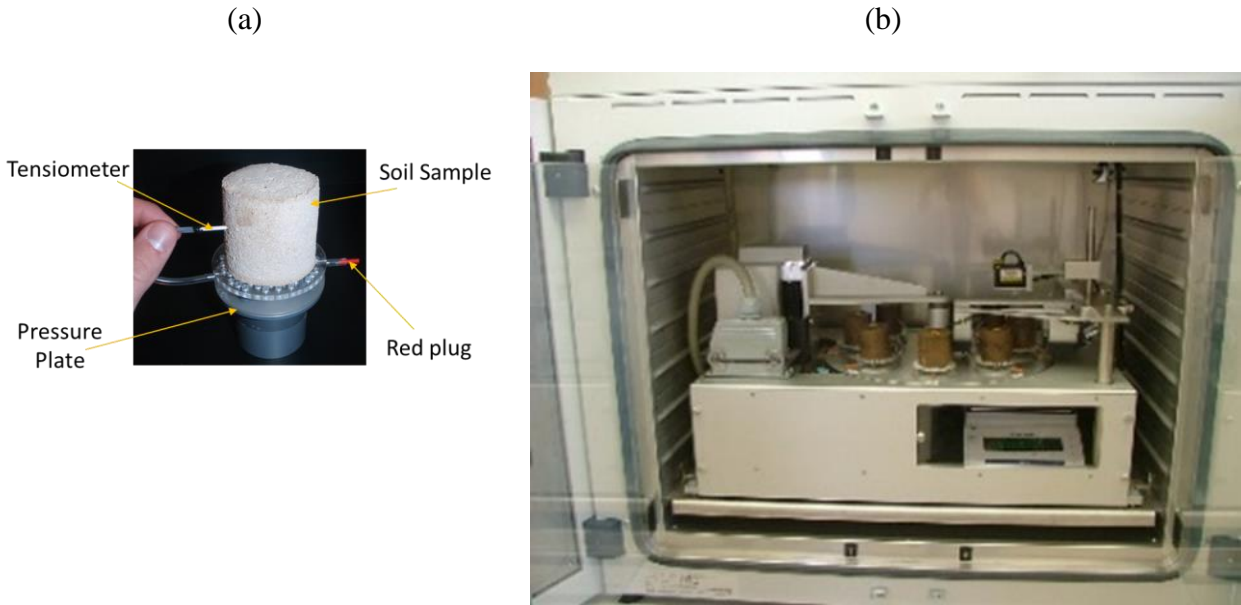


Figure 2: (a) Sample Preparation; (b) TypoSoil™ Device.

Preparation for TypoSoil™

The first step in preparing soil cores for the TypoSoil™ was to saturate them with water. For the soil cores other than the control, CeO₂-NPs⁻ were added into the space surrounded by duct tape via a beaker rather than a syringe to assure a precise, steady addition of nanoparticles. The duct tape helped simulate nanoparticles entering the system through the ground's surface. The samples were then left for 24 hours between each cycle in order to fully saturate the core with CeO₂ NPs⁻. Once the cycles were complete, the soil cores were transferred to the sand saturation cylinders to fill any available space in the soil core with water (from an inch below the

ground up to the soil surface). See Table 2 for the appropriate number of cycles and measurements of CeO₂ NPs⁻.

Table 2. CeO₂ NP⁻ Totals for Each Concentration and Cycle Repetition

Concentration of CeO₂ (mg/L)	# Cycles	Total Amount CeO₂ added (mL)	Total CeO₂ added (mg)
Control - 0	0	0	0
1 st - 500	3	150	75
1 st - 2000	3	150	300
2 nd - 500	6	300	150
2 nd - 2000	6	300	600
3 rd - 500	12	600	300
3 rd - 2000	12	600	1200

Next, any and all water² involved was degassed. Degassing the water that enters the tensiometer is important because if air gets into either the tensiometer, the tube connected to the soil sample, or the pressure plate, then tensiometer will simply reads the air pressure instead of the soil-water suction. The degassing process begins with boiling of water to remove the dissolved gas through evaporation. When the boiled water was stored and then came to room temperature, the procedures of the TypoSoilTM manual (Braudeau et al., 2015) were followed to degas the water. The procedures include using a 20 mL syringe, filling it with 5 mL and pulling the syringe in order to create a vacuum then remove the air by pressing back the syringe. I waited

² Any and all water involved in the soil samples and TypoSoilTM process was distilled water.

until all the gas was out of the water, then attached a small tube and a tensiometer to the opening of the syringe, allowing as little air in the system as possible. Then, the tensiometer was submerged in degassed, distilled water, and pulled back on the syringe again. This time waiting for all air bubbles to leave the tensiometer. Once the tensiometers were degassed, they were set aside (still submerged in water) to be attached to the pressure plates.

Similarly, the procedures of Braudeau et al., (2015), to degas the pressure plates that read the soil suction were followed. The procedures include attaching one end of each plate with a long yellow tube and placed the end in water. On the other side, I removed the red plug and attached one of the syringes with a long tube. Next, I pushed and pulled the syringe to make all the air inside of the plate escape to the atmosphere, through the yellow tube, so that only water was left in the plate. I attached one tensiometer to the tube in the water and placed the red plug back in the side that had the syringe. With the preparation of each plate done, I taped the tensiometer to the top of the plate and ran the test cycle in the TypoSoil™. The test cycle gave me the original tare weights (g) and tensiometer readings (pts.) of each pressure plate (Figure 2a).

Provided the data, I took out the plates and placed the saturated soil cores on top. I then inserted the ceramic tensiometers into the middle of each core and placed the entire plate with the soil core back into the TypoSoil™. I began the cycle and adjusted the positions of the cores based on the balance and tensiometer readings, then made sure the TypoSoil™ was recording all the appropriate readings.

Soil cores enter the apparatus saturated, are dried at a constant 40.0 degrees Celsius, and once they no longer show a change in the water content and volume. This point is an indicator that the TypoSoil™ measurement cycle is ended. Then, a user need to stop the device save the

excel sheets (reading) take the soil samples and dried them in an oven for 24 hours to get the dry mass weight of the soil cores. After having all of these data the user will be ready for analyzing the data. . One should keep in mind that the main output of the device is the measured state variables that can then be used to construct the Soil Shrinkage Curve (ShC) and the Water Retention Curve (WRC), these two curves can be used to calculate the available water capacities as well as water flow in soil medium as will be discussed in the next section.

Calculations

After all the cores completed their rounds in the TypoSoil™ machine, I downloaded the CSV files as Excel files. Each Excel file contained information for one core. The information included the core name, code, batch, date entered into the TypoSoil™, and then the time in seconds, the BARR1 and BARR2 values, the SPOT, the mass in grams, the pressure in points, and three other pressure plate values including a tension value. Each core's data was transferred to a template that compared cores exposed to the same amounts of negatively charged cerium oxide nanoparticles in order to evaluate a general trend for that particular batch.

The Excel template used for comparison analysis took the raw data of the core and automatically filled in a measured Water Retention Curve (WRC) and Soil Shrinkage Curve (ShC), a modified WRC, a modified ShC, and a formula that output the Field Capacity and Permanent Wilting Point. Even though the templates were updated automatically, I had to adjust the coefficients and standards based on my initial and recorded data. For each core I entered the appropriate dry mass weight, the maximum potential pressure and number of cycle values as well as the original pressure. On the "Mod. WRC" sheet, I adjusted validity values and other parameters such as saturation water content (W_{sat}) and coefficient values to best fit a modeled curve to the retention (h) curve. I was able to accomplish a best-fit line through the Solver

Function in Excel. I followed the same process with Solver on the “Mod. ShC” sheet. The last sheet, for FC and PWP, took the first and second minimum water content (W_{mi}) and the water content (W) and volume (V) values of the core data, and calculated the overall FC and PWP and graphed them. Recall that the Available Water Content is the difference between the Field Capacity and the Permanent Wilting Point.

At the end of each excel template of cores from the same batch is a comparison sheet. The most important data from each core is summarized on this page and is used to create a Measured Water Retention Curve (WRC) and Soil Shrinkage Curve (ShC) graph that allows for visual analysis of each soil batch. The curve increasing from left to right is the Soil Shrinkage Curve, and the curve decreasing from left to right is the Water Retention Curve. In my analysis I pay specific attention to the shape and nature of the Soil Shrinkage Curve because for a sandy soil, there is expected to be a change in slope at the end of the process where water content is low and sand particles may fall apart. Whereas, with a clayey sample, the water is held better and the specific volume does not have as noticeable a transition with low water content because it can access what it was storing within its aggregates.

CHAPTER III

RESULTS

My research studies the changes in soil-water holding properties, namely the field capacity, permanent wilting point and available water, through characterization of the properties of a sandy soil by comparing a controlled sandy soil sample with no negatively charged cerium oxide nanoparticle ($\text{CeO}_2 \text{ NPs}^-$) solution to sandy soil samples with different amounts of 500mg/L and 2000mg/L negatively charged $\text{CeO}_2 \text{ NPs}^-$. Chapter three explains the results I received from analyzing the CSV data from the TypoSoil™.

Control

The control sample was saturated only with water before entering the TypoSoil™. The major observed behavior of the control sandy soil samples was the flat shrinkage curve, which indicates a weak aggregate structure (Figure 3). However, another observation was the increase in the specific volume at the end of the shrinkage curve, this increase in the specific volume is expected in the sandy soils. As the soil gets dryer, the bond between the sand particles become weaker and starts to fall apart.

Cores 65 and 66 had pressure readings (in pts that represents the millivolt “mv”) from the high 1900s to the low 400s. The Field Capacity of the control sample was 0.142 ($\text{kg}_{\text{water}}/\text{kg}_{\text{soil}}$) and the Permanent Wilting Point was 0.109 ($\text{kg}_{\text{water}}/\text{kg}_{\text{soil}}$). Therefore, the Available Water content for the two cores was 0.033 ($\text{kg}_{\text{water}}/\text{kg}_{\text{soil}}$) (see Figure 4).

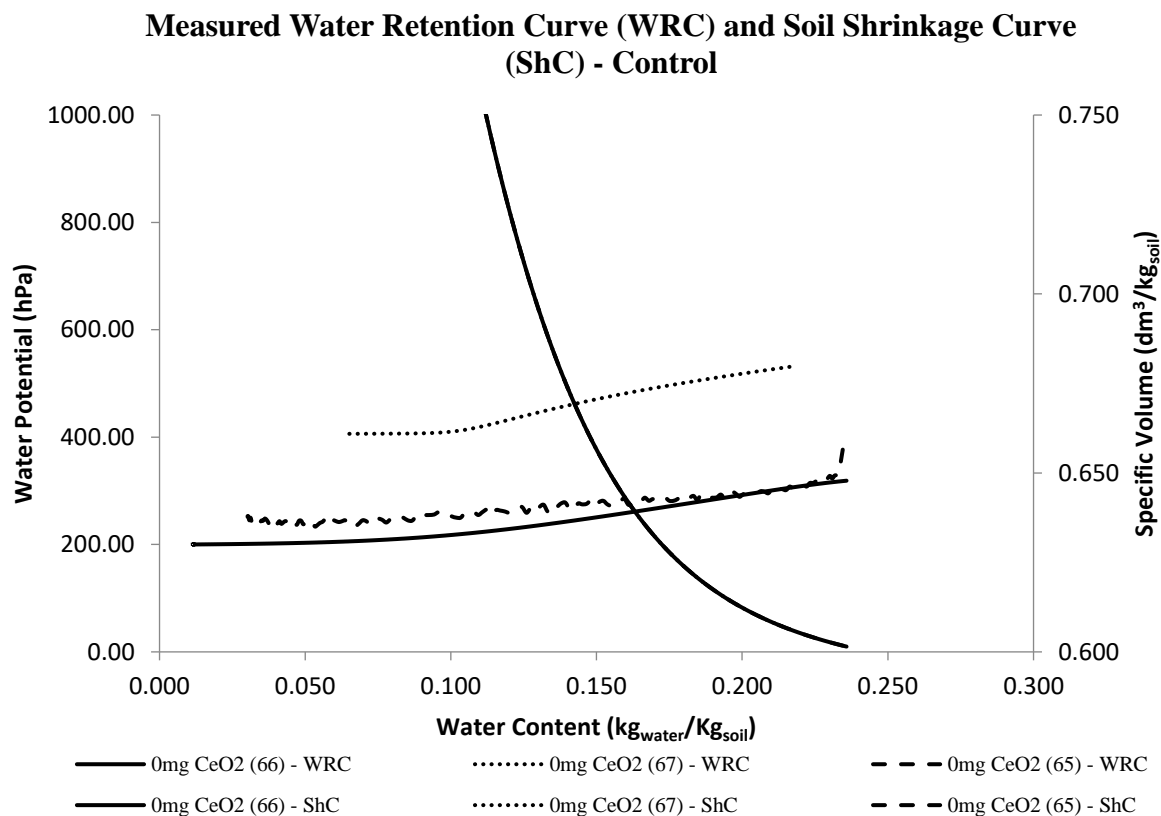


Figure 3: WRC and ShC for the Control Samples.

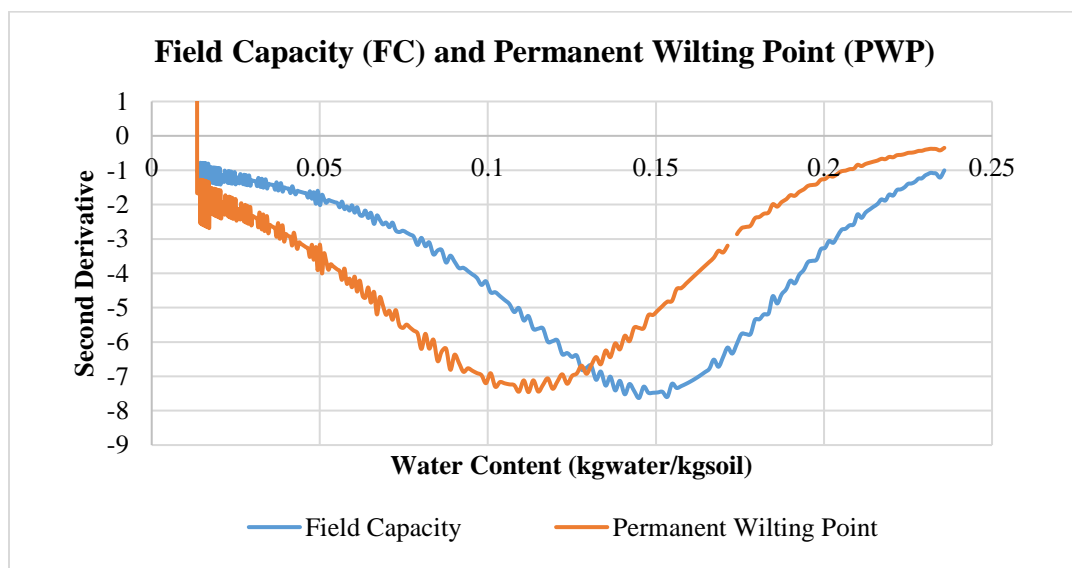


Figure 4: FC and PWP for the Control Samples.

Three Cycles

Compared to the control sample, an added 150mL of CeO₂ NPs⁻ of 500 mg/L to three cores and of 2000mg/L to another three cores resulted in an increase in water potential (hPa) and an overall lower water content range (kg_{water}/kg_{soil}).

500mg/L

Cores 52, 53, and 56 entered the TypoSoil on January 30th, 2018. Their tare weights were 385.75g, 385.91g, and 385.38g respectively. Their initial tension pressure measures were 2034pts, 2201pts, and 2008pts respectively. After taken out of the TypoSoilTM and dried, their mass weights were 146.94g, 146.84g, and 150.90g. Core 52 was the best core in terms of physical appearance, degassing, and ceramic tensiometer quality, but core 53 gave the best results in excel. Post analysis, it was difficult to remove the tensiometer from core 56 because there were large pebbles in the sample.

Cores 52 and 53 had pressure readings (in pts) from the high 1900s to the high 400s. The two cores' WRC and ShC resembled each other and can be seen in Figure 5. Core 52 had a Field Capacity of 0.201 (kg_{water}/kg_{soil}) and a Permanent Wilting Point of 0.098 (kg_{water}/kg_{soil}). Therefore, the Available Water content was 0.103 (kg_{water}/kg_{soil}).

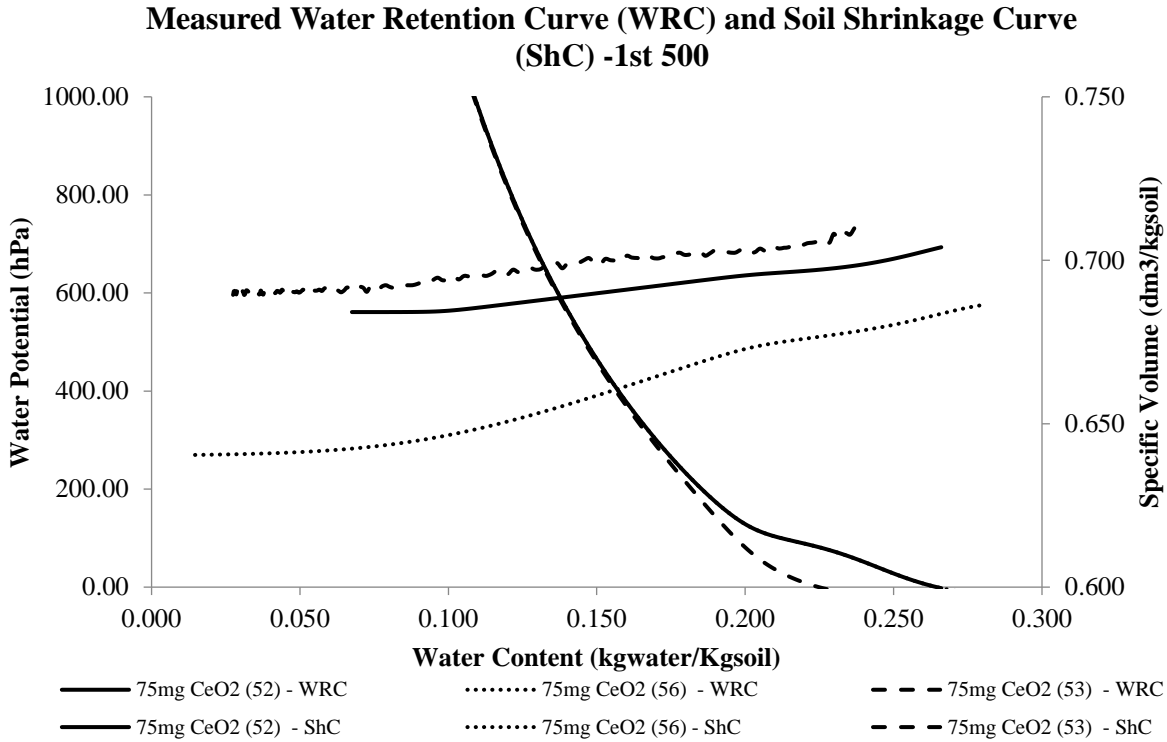


Figure 5: WRC and ShC for Three Cycles of 500mg/L CeO₂ NPs.

2000mg/L

Cores 57, 59, and 62 entered the TypoSoil on January 30th, 2018. Their tare weights were 385.20g, 384.91g, and 385.52g respectively with initial tension pressure measures of 2002pts, unknown pts, and 1969pts respectively. Post drying, their masses were 148.09g, 137.91g, and 141.09g respectively. Core 59's readings were not accurate due to mechanical failure of pressure plate number six; The TypoSoil was unable to read the Tension Measure for the sixth pressure plate. However, the Excel analysis provided a WRC and ShC of the three cores with similar data (Figure 6).

Measured Water Retention Curve (WRC) and Soil Shrinkage Curve (ShC) - 1st 2000

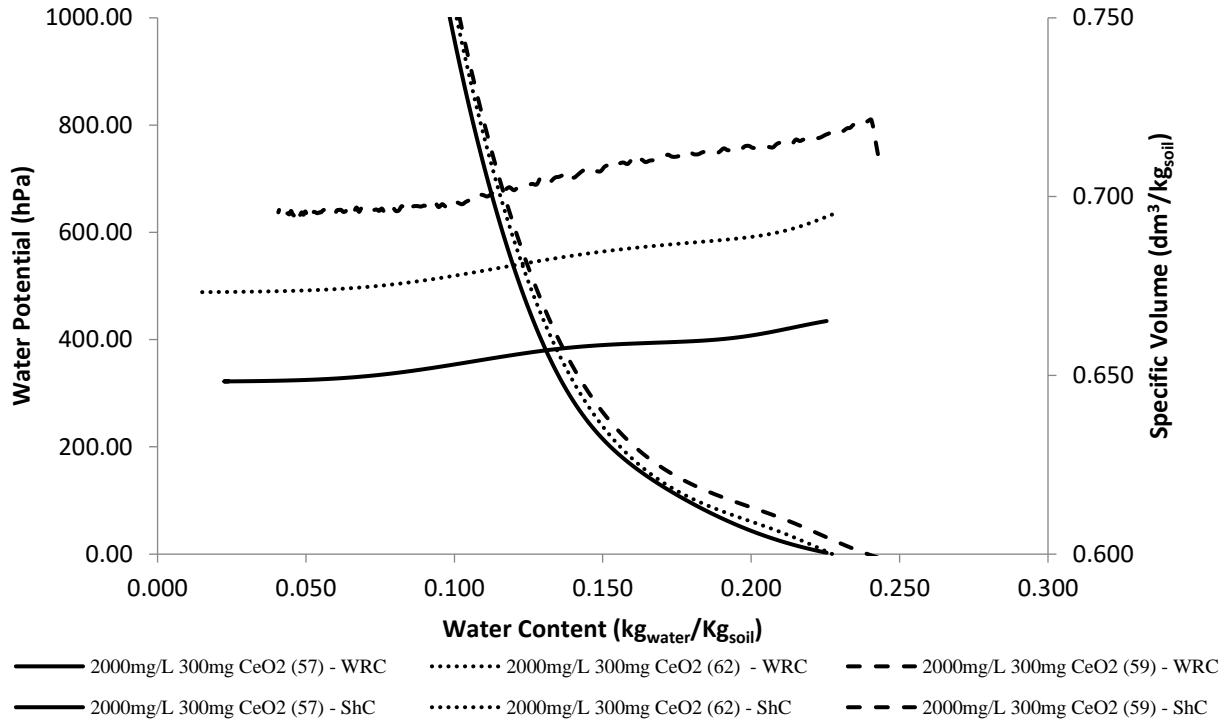


Figure 6: WRC and ShC for the Three Cores with 3 cycles of 2000mg/L CeO₂ NPs⁻.

Core 62 had the best tensiometer data and pressure readings (in pts) from the high 1900s to the low 1300s and back up to the 2000s. Therefore, core 62 is the core used in the overall comparison at the end of the conclusion, with a FC of 0.142 (kg_{water}/kg_{soil}), a PWP of 0.078 (kg_{water}/kg_{soil}), and an AW of 0.064 (kg_{water}/kg_{soil}).

Analysis

The Soil Shrinkage Curve of three cycles of 2000mg/L CeO₂ NPs⁻ began with a higher water content than the control sample did, but it still decreased with water content over time.

Six Cycles

Compared to the control sample, an added 300mL of CeO₂ NPs⁻ of 500 mg/L to three sandy soil cores and of 2000mg/L to another three cores resulted in an increase in initial water content ($\text{kg}_{\text{water}}/\text{kg}_{\text{soil}}$) and a shift in the Soil Shrinkage Curve Structure from the control values.

500mg/L

After initial tare weights and tension measures were taken, the TypoSoil™ process resulted with tare weights and tension measures of 385.73g and 1963pts, 385.82g and 1994pts, and 385.73g and 2095pts for cores 54, 69, and 55 respectively. Post TypoSoil™ and drying, the corresponding masses were 133.63g, 142.16g, and 131.81g.

Repeating the process did not solve the problem. The results for the six cycles of 2000mg/L CeO₂ NPs⁻ were inconclusive and gave neither a Soil Shrinkage nor Water Retention Curve.

2000mg/L

Cores 58, 60, and 63 entered the TypoSoil on February 20th, 2018. Respectively, their initial tare weights and tension measures were 385.95g and 1996pts, 385.96g and 1986pts, and 385.31g and 2015pts. After the process, core 58 weighed 138.58g, core 60 weighed 147.74g, and core 63 weighed 147.74g. The WRC and ShC for all three cores are graphed on Figure 7. All three cores had the same shapes for all WRCs and all ShCs, so the cores analyze with other concentrations were based on behavior I observed during the TypoSoil™ process.

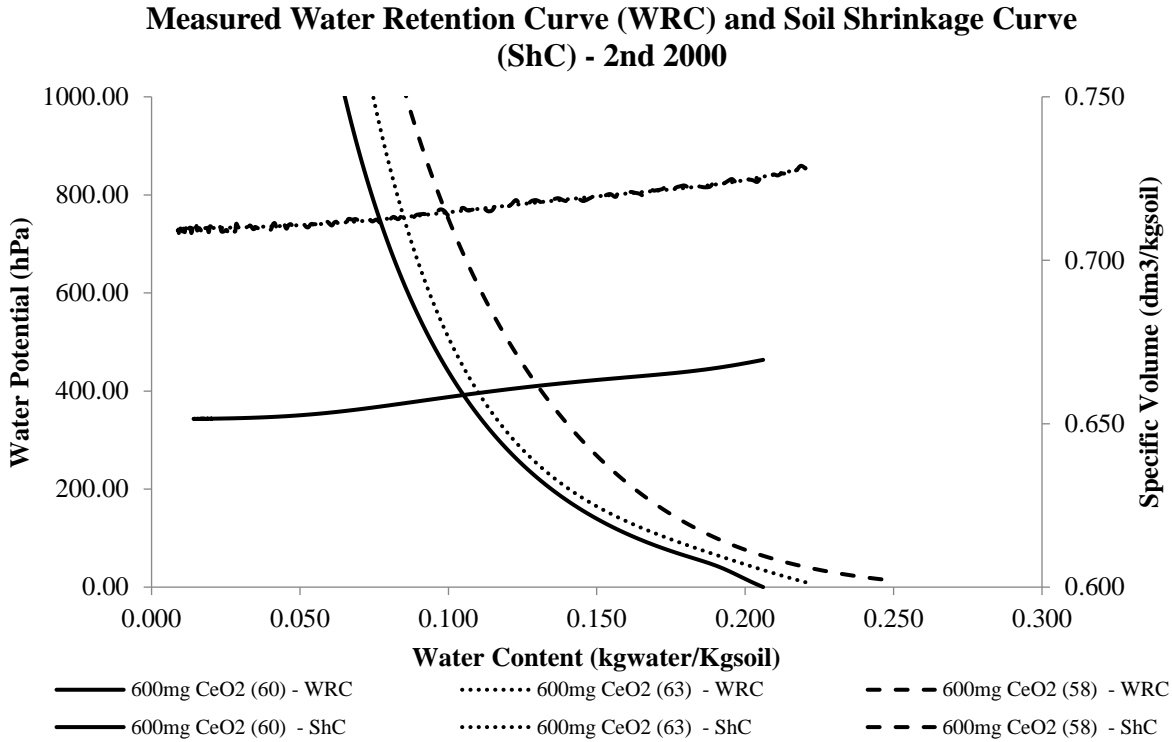


Figure 7: WRC and ShC for the Three Cores with 6 Cycles of 2000mg/L CeO₂ NP^s.

The data analysis for core 60 may have error due to the fact that during the first two cycles of adding the negatively charged cerium oxide nanoparticles, the duct tape did not hold all of the solution inside. But the four cycles after that, the solution did not leak.

Core 58 and 63 had pressure readings (in pts) from the high 1900s to the low 1300s and back up to the 2000s. Core 60 had the best readings, beginning at high 1900s and peaking at the 400s before coming back up, and will therefore be included in the concluding comparison. Core 60 had a Field Capacity of 0.185 (kg_{water}/kg_{soil}) and a Permanent Wilting Point of 0.025 (kg_{water}/kg_{soil}). Therefore, the Available Water content was 0.160 (kg_{water}/kg_{soil}).

Analysis

The measured Water Retention Curve and Soil Shrinkage Curve of six cycles of negatively charged cerium oxide nanoparticles follows the same trend set by the sandy soil

samples with the addition of three cycles of the CeO₂ NPs⁻. There is less linear trend in the ShC of the control and little to no rupture at the end of the process. Thus, indicating the addition of the increased concentration and amount of CeO₂ NPs⁻ is allowing the sandy soil to hold water longer, similar to a clayey soil sample.

Twelve Cycles

Compared to the control sample, an added 600mL of CeO₂ NPs⁻ of 500 mg/L to three sandy soil cores and of 2000mg/L to another three cores resulted in an increase in Water Potential (hPa) and a shift in the Soil Shrinkage Curve Structure from the control values. The twelve cycle samples can be compared among all the other trials. They too follow the same pattern that all the other sandy soil cores with any cycles of negatively charged cerium oxide nanoparticles have: behaving more clay-like.

500 mg/L

Cores 70, 71, and 72 had original tare weights and tension measures of 386.05g, 386.02g, 385.48g and 1978pts, 1826pts, 2006pts, respectively. After the drying process, core 70 weighed 138.71g, core 71 weighed 145.78g, and core 72 weighed 136.89g. Core 71 ended up with the most accurate TypoSoil readings, as it's tensometer reading spanned from around 2000pts to 460pts and the other readings did not go below 1000. Therefore, the complete comparison uses core 71 when referring to twelve cycles of 500mg/L CeO₂ NPs⁻. Core 71 had a Field Capacity of 0.113 (kg_{water}/kg_{soil}) and a Permanent Wilting Point of 0.039 (kg_{water}/kg_{soil}). Therefore, the Available Water content was 0.074 (kg_{water}/kg_{soil}). The Water Retention and Soil Shrinkage curves for all the cores are pictured in Figure 8.

Measured Water Retention Curve (WRC) and Soil Shrinkage Curve (ShC) -3rd 500

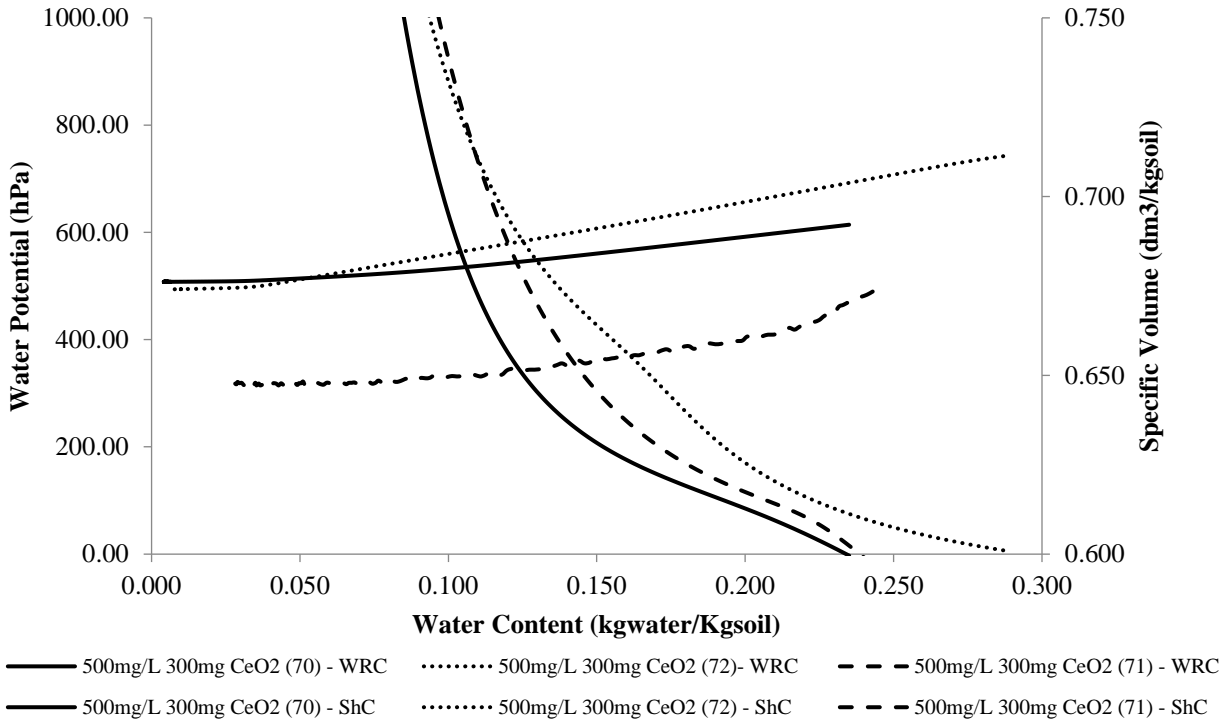


Figure 8: WRC and ShC for the Three Cores with 12 Cycles of 500mg/L CeO₂ NPs.

2000mg/L

Cores 61, 64, and 68 entered the TypoSoil™ on March 1st, 2018. Their initial tare weights and tension measures were 385.98g and 1979pts, 386.10g and 1986pts, and 385.43g and 2078pts respectively. Post TypoSoil, they weighed: 144.05g, 140.00g, and 136.42g. When preparing the tensiometers, I knew core 64 would be the best because the tensiometer degassed the best and core 68 allowed the nanoparticle solution to flow straight through it the first three cycles. Core 64 is used in the final comparison of soil shrinkage and water retention curves. Despite the differences in person, all three cores produced the same shaped Soil Shrinkage Curve (Figure 9). Core 64 had a Field Capacity of 0.169 (kg_{water}/kg_{soil}) and a Permanent Wilting Point

of 0.069 (kg_{water}/kg_{soil}). Therefore, the Available Water content was 0.100 (kg_{water}/kg_{soil}) (see Figure 10).

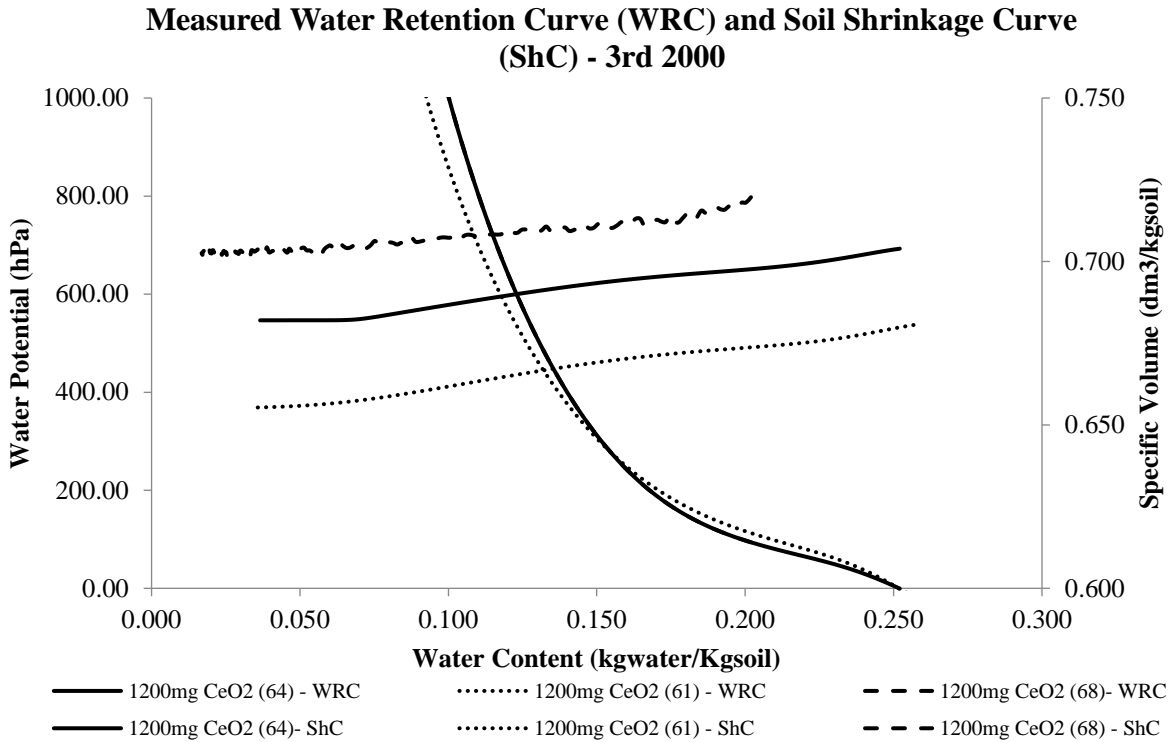


Figure 9: WRC and ShC for the Three Cores with 12 Cycles of 2000mg/L CeO₂ NPs.

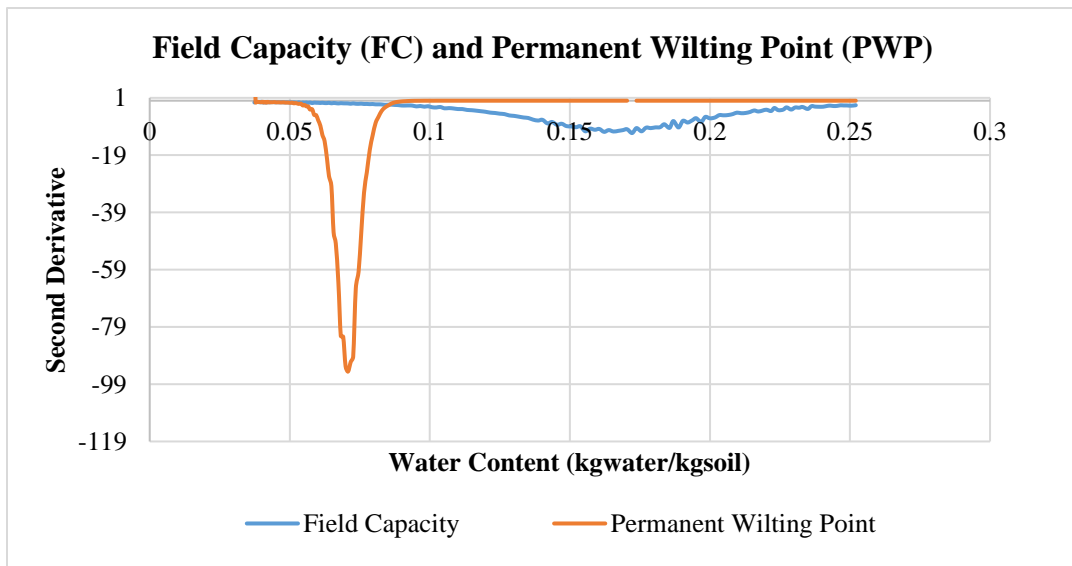


Figure 10: FC and PWP for 12 Cycles of 2000mg/L CeO₂ NPs.

Analysis

The measured Water Retention Curve and Soil Shrinkage Curve of twelve cycles of negatively charged cerium oxide nanoparticles follows the same trend set by the sandy soil samples with the various amounts of CeO_2 NPs⁻. There is less of a linear trend in the ShC of the control and practically no rupture at the end of the Soil Shrinkage Curve. Therefore, the addition of negatively charged nanoparticles to a sandy soil changes the soil's hydro-structural properties. One interesting thing about the 12 cycles of 2000mg/L CeO_2 NPs⁻ is how the Measured Water Retention Curve and Soil Shrinkage Curves turned out compared to the control samples. The next chapter will reflect on and conclude these findings.

CHAPTER IV

CONCLUSION

In the results section, the measured Water Retention Curves and the Soil Shrinkage Curves for each core that was analyzed in the TypoSoil™ was presented except for the three that gave inconclusive results (two cycles of 500mg/L CeO₂ NPs⁻). From each of the five acceptable batches and the control run, I took the best core's original excel data including their Water Potential (hPa), their Water Content (kg_{water}/kg_{soil}), and their Specific Volumes (dm³/kg_{soil}), to compile all six WRCs and ShCs onto Figure 11. The blue curves represent the soil samples exposed to twelve cycles of negatively charged cerium oxide nanoparticles and the lowest, solid, black curve (physically) on the graph is the control sample's ShC.

From Figure 11 we see that the ShC becomes with higher shrinkage amplitude, thus developing a slightly better structure of the sandy type of soil, with the increase of negatively charged cerium oxide nanoparticles. Further down the curve, there is no longer a rupture, therefore indicating that the soil is holding on to the water near the end of the process to stay attached instead of letting all water and falls apart. The soil becomes more clay-like and the available Water Content of the control is lower than that of the higher concentrations of CeO₂ NPs⁻.

When looking specifically at the 1200mg CeO₂ NPs⁻ compared to all the other ShCs on the graph, not only are the water content values higher overall, but the curve has no rupture at the end and the slope is more linear than being flat.

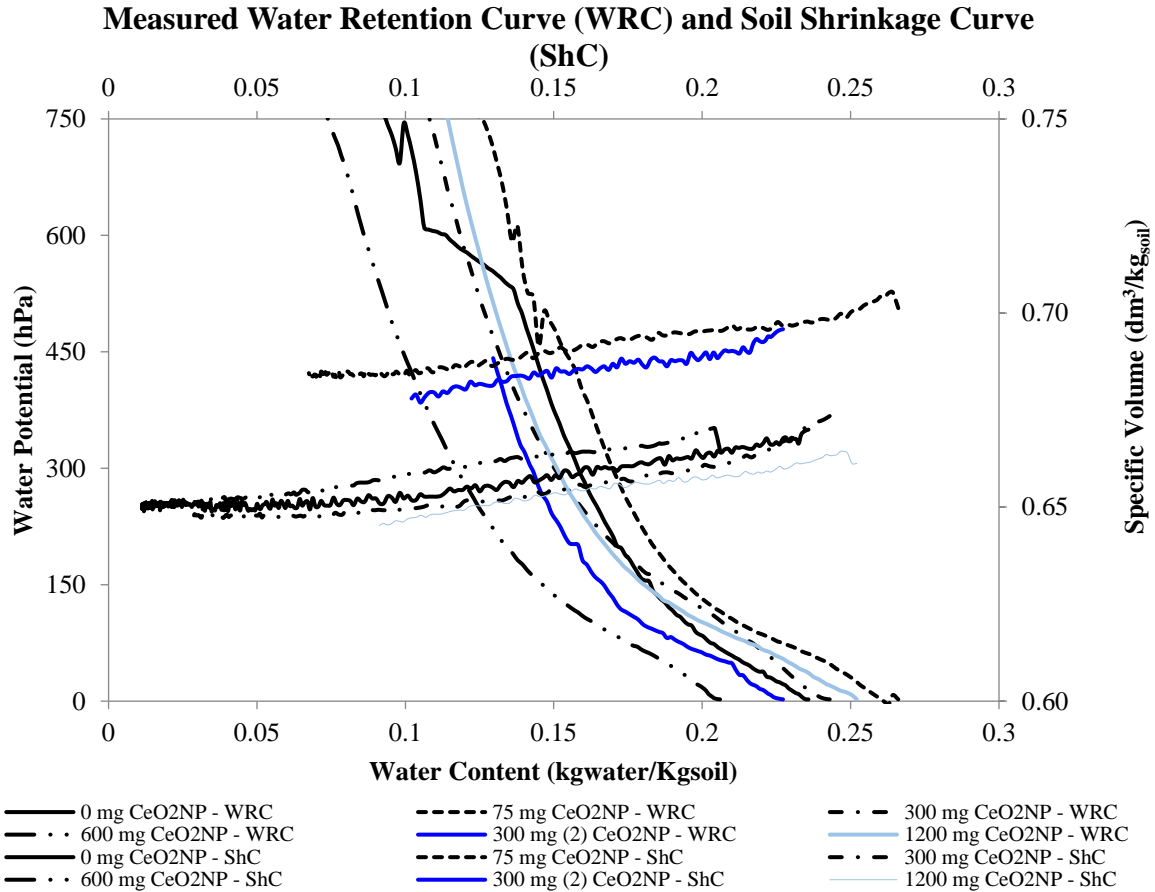


Figure 11: Combined WRC and ShC For All Conclusive Data.

Without the graphical method, one can conclude that the addition of negatively charged nanoparticles (specifically cerium oxide) results in a more clay-like characteristic of water holding properties from the resulting available water content. As described in the results, the available water content began as 0.033 (kg_{water}/kg_{soil}) with the constants and grew with the addition of nanoparticles. The largest amount of added engineered nanoparticles, 1200mg CeO₂ NPs⁻, giving an available water content of 0.100 (kg_{water}/kg_{soil}). With a higher water holding capacity, the sandy soil becomes more like a clayey soil.

Knowing that the increase in CeO₂ NPs⁻ allows for a sandy soil to behave clay-like, even if the available water decreases, there is potential for the water to still be held on top of the surface rather than flowing out with gravity. Therefore, if an engineer was working on a

remediation project and the site's soil is sandy, instead of replacing the soil with a metal or other reinforcement, the engineer could potentially add negatively charged nanoparticles to produce a similar result. To be certain on its implications, there needs to be more research done on large-scale applications.

REFERENCES

Allen, R. G., Pereira, L. S., Raes, D., and Smith, M. (1998). Crop evapotranspiration: Guidelines for computing crop requirements. *Irrigation and Drainage Paper No. 56, FAO*, (56), 300.

Assi, A.T., Blake, J., Mohtar, R.H., and Braudeau, E. (2018, submitted). Thermodynamic characterization of the soil-water holding properties using the pedostructure concept.

Assi, A.T., Accola, J., Hovhannissian, G., Mohtar, R.H., and Braudeau, E. (2014). Physics of soil medium organization, Part 2: pedostructure characterization through measurement and modeling the soil moisture characteristic curves, *Front. Environ. Sci.*, 2:5.

Belhaj, D., Jerbi, B., Medhioub, M., Zhou, J., Kellel, M., Ayadi, H., (2016). Impact of treated urban wastewater for reuse in agriculture on crop response and soil ecotoxicity. *Env. Sci. Pollu. Res.*, 23(16), 877-887.

Braudeau, E., Sene, M., and Mohtar, R.H. (2005). Hydrostructural characteristics of two African tropical soils. *Eur. J. Soil Sci.* 56, 375–388.

Braudeau, E., Assi, A.T., Boukcim, H., and Mohtar, R.H. (2014). Physics of soil medium organization, Part 1: thermodynamic formulation of the pedostructure water retention and shrinkage curves, *Front. Environ. Sci.*, 2:4.

Braudeau, E., Assi, A.T., Accola, J., Mohtar, R.H. (2015). TypoSoil™ User Manual – For Soil Hydrostructural Characterization. DOI: 10.13140/2.1.2605.3920.

Braudeau, E., Assi, A.T, and Mohtar R.H. (2016). Hydrostructural Pedology. Wiley-ISTE. 186 pages. ISBN: 978-1-84821-994.

Li, Dingsheng. (2015). *A Physiologically Based Pharmacokinetic Model Study of the Biological Fate, Transport, and Behavior of Engineered Nanoparticles*, University of Michigan, Ann Arbor, *ProQuest Dissertations & Theses Global*

Feriancikova, Lucia. (2014). "The Spread of Emerging Contaminants in the Soil-Groundwater System". *Theses and Dissertations*. 624.

Ma, Y., P. Zhang, Z. Zhang, X. He, Y. Li, J. Zhang, L. Zheng, S. Chu, K. Yang, Y. Zhao and Z. Chai (2015). Origin of the Different Phytotoxicity and Biotransformation of Cerium and Lanthanum Oxide Nanoparticles in Cucumber. *Nanotoxicology* 9(2): 262-270.

Mohd, Anuar, Mohd F. (2016). *Effects, Fate and Uptake of Nanopesticides in the Terrestrial Environment*, The University of York (United Kingdom), Ann Arbor. *ProQuest Dissertations & Theses Global*

Mohtar, R.H., Assi, A. T. and Daher, B. T. (2015). Bridging the Water and Food Gap: The Role of the Water-Energy-Food Nexus. UNUFLORES Working Paper Series 5, Edited by Hiroshan Hettiarachchi. Dresden: United Nations University Institute for Integrated Management of Material Fluxes and of Resources (UNU-FLORES).

Olar, Radu. (2017). “Nanomaterials and Nanotechnologies for Civil Engineering.” *Bulletin of the Polytechnic Institute of Jassy – CONSTRUCTIONS ARCHITECTURE Section*, pp. 109-118.

Oyanedel-Craver, Vinka (2016). “Environmental Engineering Applications of Nanoparticles.” *University of Connecticut, School of Engineering*.

Padmanabhan, G. (2014). “APPLICATION OF NANOTECHNOLOGY IN CIVIL ENGINEERING.” *The Constructor*, 22 Sept. theconstructor.org/concrete/application-of-nanotechnology-in-civil-engineering/5225/.

Rico, Cyren M. (2014) *Effects of Cerium Oxide Nanoparticles in Cereals: Insights into the Toxicity Mechanisms and Macromolecular Modifications*, The University of Texas at El Paso, Ann Arbor, *ProQuest Dissertations & Theses Global; SciTech Premium Collection*.

Veihmeyer, F. J., & Hendrickson, A. H. (1931). The moisture equivalent as a measure of the field capacity of soils. *Soil Science*.

Zacharias, S., and Bohne, K. (2008). Attempt of a flux-based evaluation of field capacity. *J. Plant Nutr. Soil Sci.*, 171(3), 399–408.

Zheng, Xianglei. (2016). *Applications of Nanotechnology in Geotechnical Engineering*, Arizona State University, Ann Arbor, *ProQuest Dissertations & Theses Global*.